Synthesis, crystal structures and catalytic oxidation of aromatic hydrocarbons by oxovanadium(V) complexes of aminebis(phenolate) ligands

Dipankar Maity [a], Jaromir Marek [b], W.S. Sheldrick [c],
H. Mayer-Figge [c], Mahammad Ali [a],*

[a] *Department of Chemistry, Jadavpur University, Kolkata 700 032, India*
[b] *X-ray Laboratory of Faculty of Science, Masaryk University, Kamenice 5, CZ 625 00 Brno, Czech Republic*
[c] *Ruhr-Universitat Bochum Lehrstuhl fur Analytischie Chemie, D-44 780 Bochum, Germany*

Abstract

The coordination chemistry of two aminebis(phenolate) ligands (H_2L^1 and H_2L^2) around vanadium(V) is described. Vanadium(V) oxo complexes (**1**, **2** and **3**) of all the ligands were obtained readily by the reaction between the ligand precursors and $[VO(acac)_2]$. Single crystal X-ray structure analysis showed that all of the complexes are penta-coordinated with trigonal bipyramidal geometry in NO_4 coordination environment. The tripodal nitrogen atom of the respective ligands and monodentate alkoxo group occupy apical positions. These complexes structurally resemble very closely to the active sites of vanadium haloperoxidases (VHPO) and were found to catalyze the oxidation of toluene to benzoic acid and isomers of xylene to the corresponding hydroxy acids with turn over numbers ranging between 134 and 188. Based on mass spectra the mechanism of the catalytic process was proposed to proceed through the formation of hydroxo–hydroperoxo intermediate, which is different from halo peroxidase reactions.
© 2007 Elsevier B.V. All rights reserved.

Keywords: Aminebis(phenolate) ligands; Trigonal bipyramidal geometry; Catalytic oxidation; Toluene and xylenes; Hydroxo–hydroperoxo intermediate

1. Introduction

The interest in vanadium chemistry both from biological and pharmacological perspectives has exploded over the past 25 years because of the discovery of the role of vanadium as an insulin mimic, and the presence of vanadium in certain haloperoxidases and nitrogenases (*Azotobacter chroococcum* and *Azotobacter vinelandii*) [1,2]. In an attempt to gain an insight into the biological roles of vanadium, many recent studies have been focused on the coordination chemistry of this metal as well as their reactivity in the oxidation states +3, +4 and +5, with biologically relevant ligands [3,4].

Inorganic vanadium(V) peroxo-complexes, some of which have been suggested to be functional models for the vanadium peroxidases [5], mediate oxygen-transfer reactions to

a variety of organic compounds including sulfides [6]. Several chiral Schiff-base-ligated vanadium(V) peroxo-complexes catalyze the formation of optically active sulfoxides, with selectivities up to 78% enantiomeric excess [7,8]. It has recently been demonstrated that the vanadium haloperoxidases are also capable of mediating selective sulfoxidation reactions in the presence of hydrogen peroxide [9–11]. Vanadium bromoperoxidase (VBPO) from the brown seaweed *Ascophyllum nodosum* promotes formation of the (*R*)-enantiomer of the methyl phenyl sulfoxide with 91% enantiomeric excess under optimal reaction conditions, whereas VBPO from the red seaweed *Corallina pilulifera* mediates formation of the (*S*)-enantiomer with 55% enantiomeric excess.

Soil and sediment bacteria have been found to mineralize many organic chemicals containing one or more benzene rings [12]. In many instances the genetic information for the biodegradative process is harbored by plasmids, which act as efficient vehicles for the spread of such information. The TOL (toluene biodegradation) plasmid of *Pseudomonas*

putida is the most extensively characterized catabolic plasmid; it encodes enzymes for the mineralization of toluene, *m*- and *p*-xylene, *m*-ethyltoluene and 1,3,4-trimethylbenzene [13,14]. In the degradation of these compounds, the methyl group at carbon-1 in the aromatic ring is sequentially oxidized to yield the corresponding carboxylic acid. The carboxylic acid is then oxidized to its corresponding catechol, which undergoes meta fission to produce a semialdehyde, which is further transformed into products, e.g., pyruvate plus aldehydes [15].

Chemical catalytic oxidation of hydrocarbon to their alcoholic, phenolic, carbonyl or carboxylic acid functions is an extremely fascinating research area [16–18], since, these are widely used as precursors for a wide variety of organic synthesis in the laboratory as well as in the industry. In this respect, very recently it has been observed that many transition metal complexes, in combination with various oxidizing agents, can catalyze the conversion of a wide variety of hydrocarbons including lower alkanes [18,19]. More specifically, oxoperoxo molybdenum(VI) complexes, in presence of H_2O_2, catalyze the oxidation of alkyl benzenes [20]. On the contrary, vanadium compounds have been widely used as catalyst in H_2O_2 as well as O_2 oxidation of hydrocarbons [16,17,21], but so far yields and TON (turn over number) obtained are not very remarkable. Barnhard and Huged used vanadium complexes as catalyst, but the assistance of a reducing agent, namely, substituted hydrocarbons, in high amount was necessary [22], which makes the process less cost-effective.

It has been observed previously that vanadium(V) as well as group-4 metal complexes of tri- (ONO) and tetra- (ONNO) dentate aminebis(phenolate) ligand have proved to be highly active olefin polymerization catalysts [23–25]. Again, [VO(ONO)] complexes of two aminebis(phenol) ligands (H_2L^1 and H_2L^2) resemble closely with the recently reported active sites in vanadium haloperoxidases (Scheme 1) [26].
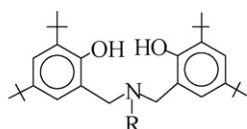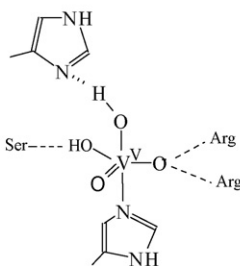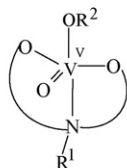
All these lead us to design and synthesize structural and functional models of the biomolecules, which has the potential ability to catalyze hydrocarbon oxidation. The model complexes described here, are believed to catalyze the oxidation of aromatic hydrocarbon through the formation of hydroxo–hydroperoxo [V(ONO)(OH)(OOH)(OMe)] intermediate. We report here the synthesis, crystal structures (**1–3**) catalytic oxidation of aromatic hydrocarbons by H_2O_2.

2. Experimental

2.1. Physical measurements

Elemental analyses were carried out using a Perkin-Elmer 240 elemental analyzer. Infrared spectra (400–4000 cm^{-1}) were recorded from KBr pellets on a Nickolet Magna IR 750 series-II FTIR spectrophotometer. Electronic spectra were recorded from Agilent 8453 UV–vis diode array Spectrophotometer. Mass spectra were recorded on a Micromass Q-TOF spectrometer with electron spray ionization source. Electrochemical measurements were carried out using a computer controlled PAR model 263A VERSASTAT electrochemical instruments with Platinum working electrode and saturated calomel electrode (SCE) as reference one.

2.2. Materials

Starting materials for the synthesis of ligands (H_2L^1) and (H_2L^2), namely, 2,4-di-*tert*-butylphenol (Lancaster), formaldehyde (Merck India), *n*-butylamine (Loba Chemie, India), *n*-propylamine (Loba Chemie, India), are of reagent grade and used as received. Solvents like methanol, ethanol, petroleum ether, acetonitrile (Merck India) were of reagent grade and dried by standard methods before use. Substrates namely toluene and isomers of xylene (Merck India) used in the catalytic reaction are of spectroscopic grade and used as received. Thirty percent of H_2O_2 (Merck India) was used in the catalytic oxidation reactions.

2.3. Synthesis of the ligands

The ligands (H_2L^1 and H_2L^2) have been synthesized according to the published procedure [27] and further characterized by CHN and NMR spectroscopic analysis.

2.4. Preparation of the complexes

2.4.1. General methods for the synthesis of complexes (**1**), (**2**) and (**3**)

[VO(acac)$_2$] (1.0 mmol, 0.256 g) was dissolved in appropriate alcohol and equimolar quantity of the respective ligand (H_2L^1 or H_2L^2) dissolved in the same solvent was added to it and refluxed for 2 h. On cooling to room temperature the suspended material initially formed was filtered off and the filtrate was subjected to slow evaporation at room temperature whereupon dark brown crystals suitable for X-ray study were obtained within a week.

H$_2$L^1: R = *n*-butyl
H$_2$L^2: R = *n*-propyl

Active center for vanadate-dependent
bromoperoxidase

complex **1**, R^1= *n*-butyl , R^2 = Me;
complex **2**, R^1 = *n*-propyl, R^2 = Me
complex **3**, R^1 = *n*-propyl, R^2 = Et

Scheme 1. .

- [$V^VO(L^1)(OMe)$] (**1**). Yield, 86%. Anal. Calc. for $C_{35}H_{56}NO_4V$: C, 69.42%; H, 9.26%; N, 2.31%. Found: C, 69.25%; H, 9.20%; N, 2.35%. FTIR (KBr disc; cm^{-1}) ν(V=O) 966.
- [$V^VO(L^2)(OMe)$] (**2**). Yield, 85%. Anal. Calc. for $C_{34}H_{54}NO_4V$: C, 69.04%; H, 9.14%; N, 2.37%. Found: C, 68.87%; H, 9.25%; N, 2.45%. FTIR (KBr disc; cm^{-1}) ν(V=O) 970.
- [$V^VO(L^2)(OEt)$] (**3**). Yield, 84%. Anal. Calc. for $C_{35}H_{56}NO_4V$: C, 69.42%; H, 9.26%; N, 2.31%. Found: C, 69.21%; H, 9.25%; N, 2.40%. FTIR (KBr disc; cm^{-1}) ν(V=O) 972.

2.5. X-ray crystallography

Intensity data for [$V^VO(L^1)(OMe)$] (**1**) were collected at 293(2) K on a smart CD defractometer using graphite monochromatized Mo Kα radiation ($\lambda = 0.71073$ Å and the $\omega - 2\theta$ scan mode in the range $2.75 < 2\theta < 27.50°$). No decomposition of the crystal occurred during the data collection. The intensities were corrected for Lorentz and polarization effects and for absorption using the ψ-scan data. The structure was solved by direct methods using SHELXS-97 [28] and was refined anisotropically on F^2 using the full-matrix least-squares procedure of SHELXL-97 [29] and hydrogen atoms were included in the model at their calculated positions with d(C–H = 0.93–0.97 Å) and U_{iso}(H) values of 1. Five equivalents of (C) for methyl protons and 1.2 equiv. (C) for other protons at convergence [σ weights, i.e., $1/\sigma^2(F)$],

$R_1 = 0.054$ and $wR_2 = 0.143$ for **1** [$I > 2\sigma(I)$]; final refinement details are given in Table 1. The maximum peak in the final difference map was 0.87 e Å^{-3} the minimum peak -0.22 e Å^{-3}.

The diffraction data for complexes **2** and **3** were collected with a KM4CCD diffractometer with a four-circle area-detector (KUMA Diffraction, Poland), and equipped with an Oxford Cryostream Cooler (Oxford Cryosystems, UK). Mo Kα radiation (monochromator Enhance, Oxford Diffraction, UK) was used in all measurements. The ω-scan technique with different κ and φ offsets for covering an independent part of reflections in the 3.2–25.0° θ range was performed. The cell parameters were refined from all strong reflections. The data reductions were carried out using the CrysAlis RED (Oxford Diffraction, UK) program, and analytical absorption corrections were applied. The structures were determined by direct methods and SHELXS-97 [28]. Both structures were refined anisotropically on F^2 using the full-matrix least-squares procedure of SHELXL-97 [29]. H atoms attached to C atoms were positioned geometrically, with C–H = 0.95–0.98 Å, and with U_{iso}(H) values of $1.2U_{eq}$(C) [1.5 U_{eq}(C) for methyl atoms]. The data for publication were prepared by SHELXL and PARST [30] and the figures by ORTEP-III [31]. The crystal and the procedure for data refinement are listed in Table 1 for all three complexes.

2.6. Experimental set up for catalytic oxidation

A mixture of complex **2** (the catalyst) (0.0592 g, 0.10 mmol), a representative substrate, namely toluene (20 mmol), was

Table 1
Summary of crystallographic data

	Complex		
	1	**2**	**3**
Empirical formula	$C_{35}H_{56}NO_4V$	$C_{34}H_{54}NO_4V$	$C_{35}H_{56}NO_4V$
Formula weight	605.75	591.72	605.75
Temperature (K)	293(2)	120(2)	426(2)
Wavelength (Å)	0.71073	0.71073	0.71073
Crystal system	Monoclinic	Monoclinic	Monoclinic
Space group	$P2_1$	$P2_1$	$P2_1$
Unit cell dimensions			
a (Å)	10.582(3)	10.400(8)	0.201(7)
b (Å)	15.270(3)	14.923(12)	15.565(10)
c (Å)	11.148(3)	11.221(9)	11.194(8)
β (°)	102.52(3)	103.211(8)	104.108(7)
Volume (A^3)	1758.5(8)	1695.4(2)	1723.6(2)
Z	2	2	2
ρ_{calc} (g/cm^3)	1.127	1.159	1.167
μ (mm^{-1})	0.316	0.327	0.323
Maximum and minimum transmission	0.687 and 0.647	0.938 and 0.894	0.9381 and 0.8815
Crystal size (mm^3)	$0.35 \times 0.51 \times 0.60$	$0.20 \times 0.30 \times 0.35$	$0.20 \times 0.40 \times 0.40$
θ limit (°)	2.75–27.5	3.31–25	3.22–24.99
Index ranges (h; k; l)	$-1, 13; -1, 19; -14, 14$	$-12, 12; -17, 16; -13, 12$	$-12, 12; -18, 18; -13, 12$
Reflections collected	5105	9723	10348
Independent reflections	4423	5305	5679
Observed reflections [$I > 2\sigma(I)$]	3572	4389	4725
Data/restraints/parameters	4423/24/379	5305/1/375	5679/1/384
Goodness-of-fit-on F^2	1.04	0.98	0.93
Final R indices [$I > 2\sigma(I)$]	$R_1 = 0.0540, \omega R_2 = 0.1567$	$R_1 = 0.0532, \omega R_2 = 0.1318$	$R_1 = 0.0346, \omega R_2 = 0.0615$
Largest diff. peak and hole (e A^{-3})	0.87 and -0.22	0.80 and -0.34	0.37 and -0.30

dissolved in 10 ml MeCN solvent and the resulting solution was taken in a 50 ml capacity Parr type hydrogenation apparatus. To the above solution was then added 2 ml of 30% H_2O_2 and the resulting solution turned yellow. The assembly was then plunged in water to assure that the system was airtight. The solution was then heated on an oil bath to reflux for 5–12 h as required and 0.5 ml of H_2O_2 was added intermittently at a time interval of 60 min. The reaction was quenched at a certain interval of time lowering the temperature to $-5°$ and the solution was analyzed thereafter by GC.

2.7. Recovery of catalyst

After each set of catalytic oxidation had been quenched, the reaction mixture left was thoroughly shaken with diethyl ether whereupon the substrates and the products were extracted in the ether layer almost quantitatively. The ether layer containing the catalyst, product and the unreacted substrate was separated out by a separating funnel and then added to appropriate alcohol and refluxed for 2 h in air. The resulting dark brown solution was then allowed to cool, filtered and kept for slow evaporation where upon shiny crystals of the catalyst (complex **2**) were deposited within few days. The crystals were separated by filtration and dried in air and characterized by comparing elemental as well as IR spectrum with the original complex.

3. Results and discussion

3.1. Description of the crystal structures

[VOL^1(OMe)] (**1**), [V^{V}O(L^2)(OMe)] (**2**) and [V^{V}O(L^2) (OEt)] (**3**). Crystal Structure determination of complexes **1**, **2** and **3** reveal the similar features. The asymmetric unit cells consist of discrete molecules of the complexes. The ORTEP views with atom numbering scheme of complexes **1**, **2** and **3** are shown in Figs. 1–3, respectively. Selected interatomic parameters are listed in Table 2. In each of the three cases vanadium atom adopts the relatively uncommon TBP geometry under NO_4 donor environment that usually occurs only in a sterically congested ligand environment to relieve some steric strain [32].
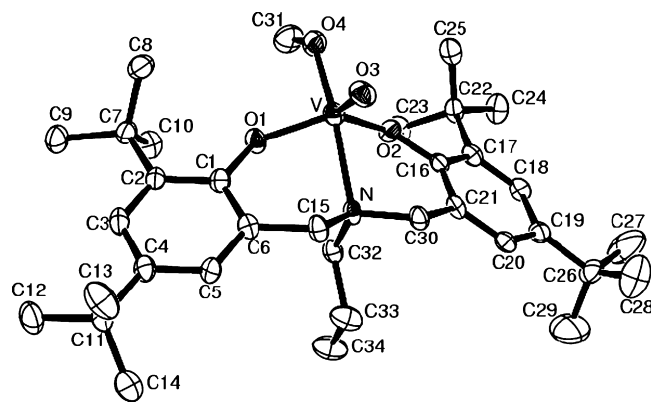

Fig. 2. ORTEP view with atom numbering scheme for complex **2** drawn at 30% probability ellipsoid. Hydrogen atoms are omitted for clarity.

In all three penta-coordinated complexes basal coordinates are occupied by phenolate oxygen atoms O(1) and O(2) of the ligand and an oxo function O(3). The tripodal nitrogen atom of the respective ligand and a monodentate alkoxo group occupy apical positions. The vanadium atoms do not lie on the O(1), O(2) and O(3) plane but are displaced slightly above the plane towards the V–O(4) bond. This deviation is fairly equal for complexes **1** and **3** with 0.193 and 0.191 Å respectively and slightly higher for complex **2** (0.20 Å). The distortion from ideal geometry may be caused by the smaller bite angles between the phenolate O atom and the imine nitrogen atom of the tridentate ligand. The O(phenolate)–V–N angles are in the order of 80.46–81.83° which are remarkably narrower than the ideal angle. V–O oxo distances are in good agreement for all three complexes but the V–N distances differ significantly in complex **3** being 2.228(2) Å whereas these distances are 2.237(4) and 2.238(3) for complexes **1** and **2** which is typical for a tertiary N atom sited axially *trans* to an oxo function [33]. The angular parameter τ calculation [34] clearly indicates that all the three structures are trigonal bipyramidal but distorted somewhat towards a square-pyramid geometry. τ values show that the H_2L^2 ligated complexes **2** and **3** (66.4% and 64.5%, respectively) are more distorted than the H_2L^1 ligated complex **1** ($\tau = 68.8\%$), but the reason for this state of affairs is not clear.
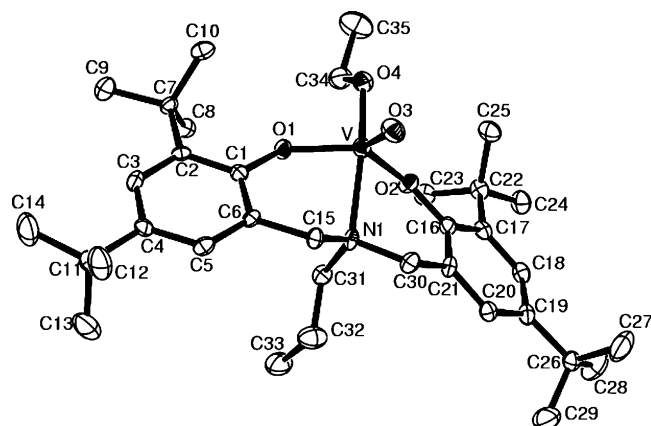

Fig. 1. ORTEP view with atom numbering scheme for complex **1** drawn at 30% probability ellipsoid. Hydrogen atoms are omitted for clarity.
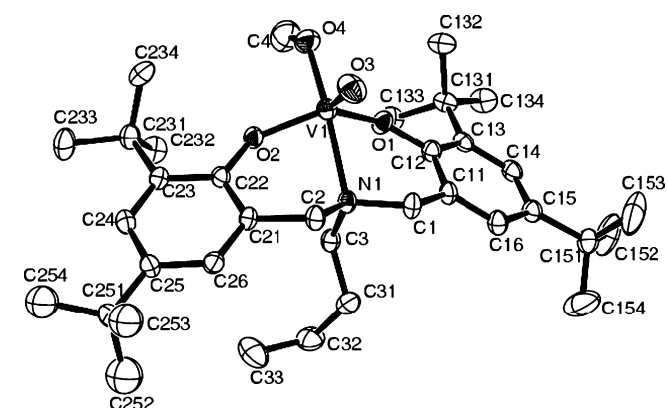

Fig. 3. ORTEP view with atom numbering scheme for complex **3** drawn at 30% probability ellipsoid. Hydrogen atoms are omitted for clarity.

Table 2
Selected bond lengths and bond angles in the complexes **1**, **2** and **3**

1	**2**	**3**
Bond length (Å)		
V(1)–O(1) 1.835(3)	V–O(1) 1.825(2)	V–O(1) 1.835(2)
V(1)–O(2) 1.832(3)	V–O(2) 1.828(2)	V–O(2) 1.833(1)
V(1)–O(3) 1.579(4)	V–O(3) 1.581(3)	V–O(3) 1.576(2)
V(1)–O(4) 1.782(5)	V–O(4) 1.798(3)	V–O(4) 1.796(2)
V(1)–N(1) 2.237(3)	V –N 2.238(3)	V–N(1) 2.228(2)
Bond angles (°)		
O(1)–V(1)–O(2) 128.65(2)	O(1)–V–O(2) 128.63(1)	O(1)–V–O(2) 128.76(7)
O(1)–V(1)–O(3) 114.16(2)	O(1)–V–O(3) 113.59(1)	O(1)–V–O(3) 113.84(8)
O(1)–V(1)–O(4) 93.78(2)	O(1)–V–O(4) 94.22(1)	O(1)–V–O(4) 93.30(8)
O(1)–V(1)–N(1) 81.63(1)	O(1)–V–N 81.18(1)	O(1)–V–N(1) 81.46(7)
O(2)–V(1)–O(3) 113.53(2)	O(2)–V–O(3) 113.82(1)	O(2)–V–O(3) 113.81(9)
O(2)–V(1)–O(4) 95.33(2)	O(2)–V–O(4) 94.21(1)	O(2)–V–O(4) 93.70(7)
O(2)–V(1)–N(1) 80.82(1)	O(2)–V–N 80.71(1)	O(2)–V–N(1) 80.96(7)
O(3)–V(1)–O(4) 100.5(2)	O(3)–V–O(4) 102.15(2)	O(3)–V–O(4) 102.79(9)
O(3)–V(1)–N(1) 89.53(2)	O(3)–V–N 89.37(1)	O(3)–V–N(1) 89.77(8)
O(4)–V(1)–N(1) 169.93(2)	O(4)–V–N 168.47(1)	O(4)–V–N(1) 167.43(8)

In all the three complexes the tridentate tripodal ligands H_2L^1 and H_2L^2 behave in a very similar way wrapping the metal center facially and the non-symmetry related phenyl rings flip back to the same side of the vanadium center giving rise to a *fac-cis* isomer in each case. All the phenyl rings retain their aromaticity and the two planes formed by the respective aromatic rings intersects at an angle of about 34° in the complexes **1** and **2** and somewhat narrower angle for **3**.

3.2. Electrochemical study

The electrochemical behavior of complex **2** was studied by cyclic voltammetry in the range +2.00 to −0.5 V at a scan rate 100 mV/s in MeCN at platinum electrode versus SCE using tetrabutylammonium perchlorate (TBAP) as supporting electrolyte. Complex **2** showed (Fig. 4) a quasi-reversible peak at −0.20 V. Controlled coulometric experiment shows that the wave is one-electron transfer process. Since the phenolate ligand as well as
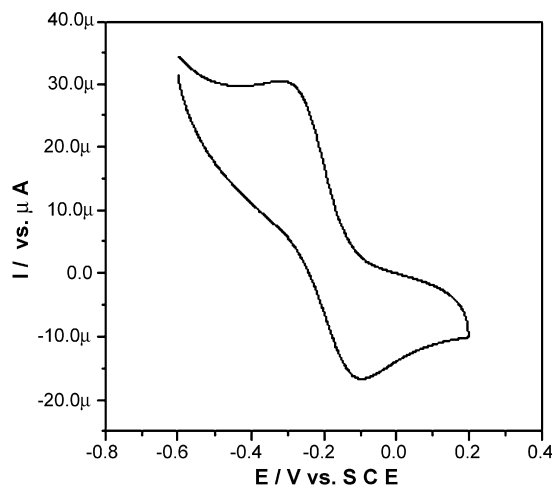
methoxy group could not be reduced in this potential range [35], we assign this as a metal centered reduction potential for the VO^{3+}/VO^{2+} couple.

3.3. Catalytic oxidation

The yield of the reaction products were monitored by GC at different times and the plots of % yield versus time (h) (Fig. 5) for three representative substrates, viz. toluene, *o*- and *p*-xylenes give reasonable straight lines for the later points, taking origin as one of the points and the rate constants evaluated to be 8.42 ± 0.43, 5.78 ± 0.30 and $7.28 \pm 0.51\,h^{-1}$, respectively. Notably, decrease in rate as well as in the product percentage from toluene to *o*-xylene (Table 3) clearly indicates that lower the steric crowding in the substrate higher is the yield of the product. The mechanism of the reaction is not fully clear. However, sensitivity of the catalytic reactions towards AIBN and benzoquinone lead us to assume a radical mechanism and the tentative sequence of reaction steps could be framed as shown
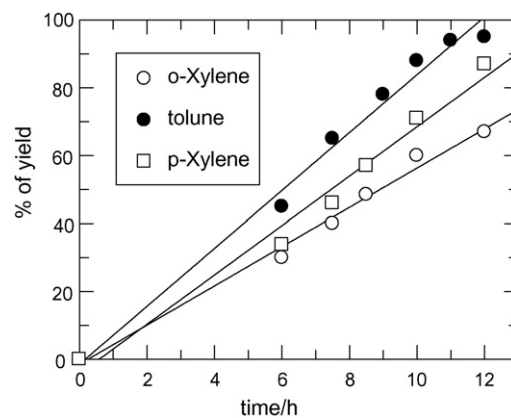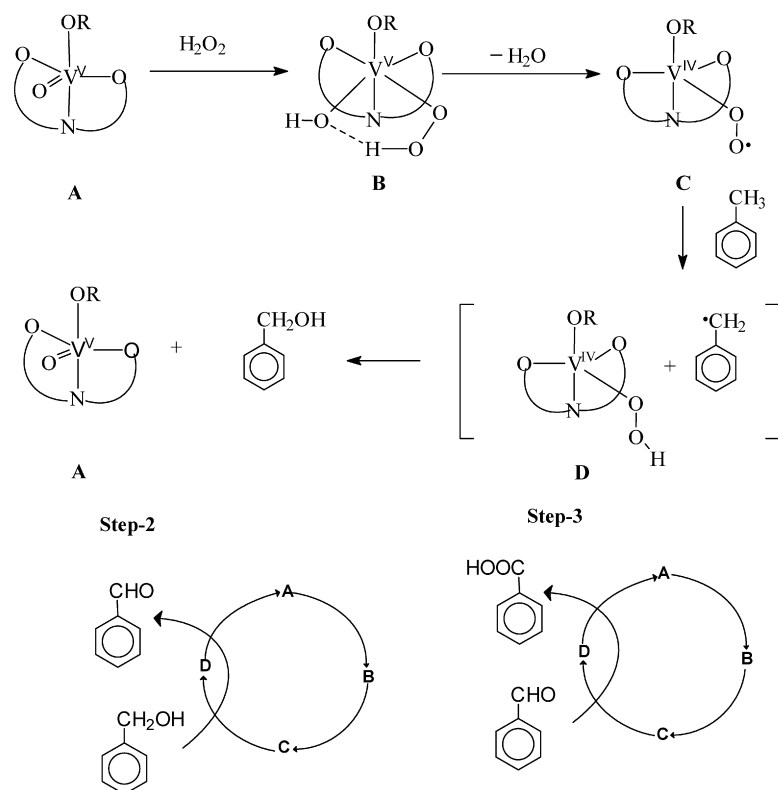

Fig. 4. Cyclic voltammogram of complex **2** in acetonitrile solution containing 1mM complex and 0.1 M *n*-Bu₄NClO₄ (scan rate = 0.1 V/s).

Fig. 5. Plots of % yield vs. time (h) for the catalytic oxidation of toluene, *o*-xylene, and *p*-xylene by H_2O_2 using complex **2** as catalyst with substrate:catalyst = 200:1.

Scheme 2. .

in Scheme 2. On addition of H_2O_2 to an acetonitrile solution of complex **2** changes from brown to green rendering an electronic transition at 531 nm ($\varepsilon = 164 \, mol^{-1} \, cm^2$), which is characteristic for a d–d transition. Cyclic voltametric study also reveals the quasi-reversible regeneration of initial complex. ESI-MS study of the toluene oxidation reaction mixture shows the existence

of benzyl alcohol and benzaldehyde and hydroxo–hydroperoxo [V(ONO)(OH)(OOH)(OMe)] species (Supplementary Fig. 1) proving the self-consistency of the proposed mechanistic pathways [18] (Scheme 2). The model complexes described here catalyze the oxidation of aromatic hydrocarbons through the formation of hydroxo–hydroperoxo [V(ONO)(OH)(OOH)(OMe)] intermediate, unlike the previously proposed mechanism of haloperoxidase reactions, where, an oxo–peroxo intermediate has been proposed [17].

Table 3
Details of catalytic oxidation of hydrocarbons by H2O2 using complex **2** as catalyst

Substrate	Product	% Yield	Turn over number	k (h^{-1})
(toluene)	COOH	94	188	8.42
(o-xylene)	COOH, CH$_2$OH	67	134	5.78
(p-xylene)	COOH, CH$_2$OH	87	174	7.28

4. Conclusion

(1) The coordination properties of two aminebis(phenolate) ligands (H_2L^1 and H_2L^2) around vanadium(V) are described here.

(2) Vanadium(V) oxo complexes [VOL^1(OMe)] (**1**), [V^{V}O(L^2)(OMe)] (**2**) and [V^{V}O(L^2)(OEt)] (**3**) were readily obtained by the simple reaction between the ligand precursors and VO(acac)$_2$ in MeCN.

(3) Single crystal X-ray structure analyses reveal that all the complexes have trigonal bipyramidal geometry under NO$_4$ coordination environment.

(4) These complexes structurally resemble very closely to the active sites of "haloperoxidases".

(5) Complex **1** showed a quasi-reversible peak at −0.20 V and corresponds to the VO^{3+}/VO^{2+} couple.

(6) These were found to catalyze the oxidation of toluene to benzoic acid and isomers of xylene to the correspond-

ing hydroxy acids with turn over numbers ~188 and hydroxo–hydroperoxo species [VOH(OOH)(L^2)(OMe)] as the active intermediate.

Acknowledgements

Appendix A

Crystallographic data have been deposited with the Cambridge Crystallographic Data Center, 12 Union Road, Cambridge CB2 1EZ, UK (fax: +44 1223 336033: e-mail: deposit@ccdc.cam.ac.uk) and are available on request quoting the deposition numbers ccdc-278611 and 278610 for complexes **2** and **3**, respectively.

Appendix B. Supplementary data

Supplementary data associated with this article can be found, in the online version, at doi:10.1016/j.molcata.2007.01.041.

References

[1] C. Slebodnick, B.J. Hamstra, V.L. Pecoraro, Struct. Bonding 89 (1997) 51.
[2] H. Sigel, A. Sigel (Eds.), Metal Ions in Biological Systems, vol. 31: Vanadium and its Role in Life, Marcel Dekker, New York, 1995.
[3] (a) J.A. Bonadies, C.J. Carrano, J. Am. Soc. 108 (1986) 4088;
(b) G.J. Colpas, B.J. Hamstra, J.W. Kampf, V.L. Pecoraro, Inorg. Chem. 33 (1994) 4669, and the references therein.
[4] A. Neves, A.S. Ceccato, C. Erasmus-Buhr, S. Gehring, G. Haase, H. Paulus, O.R. Nascimento, A.A. Batista, J. Chem. Soc. Chem. Commun. (1993) 1782, and the references therein.
[5] A. Butler, A.H. Baldwin, in: P.J. Sadler (Ed.), Metal Sites in Proteins and Models, vol. 89, Springer-Verlag, Berlin, 1997, p. 109.
[6] A. Butler, M.J. Clague, G.E. Meister, Chem. Rev. 94 (1994) 625.
[7] C. Bolm, F. Bienewald, Angew. Chem. Int. Ed. Engl. 34 (1995) 2640.
[8] A.H. Vetter, A. Berkessel, Tetrahedron Lett. 39 (1998) 1741.
[9] H.B. Ten Brink, A. Tuynman, H.L. Dekker, W. Hemrika, Y. Izumi, T. Oshiro, H.E. Schoemaker, R. Wever, Inorg. Chem. 37 (1998) 6780.
[10] H.B. Ten Brink, H.L. Holland, H.E. Schoemaker, H. van Lingen, R. Wever, Tetrahedron Asymm. 10 (1999) 4563.
[11] M. Andersson, A. Willets, S. Allenmark, J. Org. Chem. 62 (1997) 8455.
[12] D.T. Gibson, V. Subramanian, in: D.T. Gibson (Ed.), Microbial Degradation of Organic Compounds, Marcel Dekker, Inc., New York, 1984, p. 181.
[13] D.A. Kunz, P.J. Chapman, J. Bacteriol. 146 (1981) 179.
[14] M.J. Worsey, F.C.H. Franklin, P.A. Williams, J. Bacteriol. 134 (1978) 757.
[15] M.A. Abril, C. Michan, K.N. Timmis, J.L. Ramos, J. Bacteriol. 171 (1989) 6782.
[16] H. Mimoun, L. Saussine, E. doire, M. Postel, J. Fischer, R. Weiss, J. Am. Chem. Soc. 105 (1983) 3101.
[17] E. Battistel, R. Tassinari, M. Fornaroli, L. Bonoldi, J. Mol. Catal. A: Chem. 202 (2003) 107.
[18] G.B. Shulpin, G. Sürs-Fink, L.S. Shul'pina, Chem. Commun. (2000) 1131.
[19] (a) J.A.A.W. Elemeans, E.J.A. Bijsterveld, A.E. Rowan, R.J.M. Nolte, Chem. Commun. (2000) 2443, and references cited therein;
(b) R.A. Periana, D. Miranov, D. Tanbe, G. Bhalla, C.J. Jones, Science 301 (2003) 814, and references cited therein.
[20] R. Bandyopadhyay, S. Biswas, S. Guha, A.K. Mukherjee, R. Bhattacharyya, Chem. Commun. (1999) 1627.
[21] S. Das, T. Bhowmick, T. Punniyamurthy, D. Dey, J. Nath, M.K. Choudhuri, Tetrahedron Lett. 44 (2003) 4915.
[22] G.B. Shulpin, D. Atanasio, L. Suber, J. Catal. 142 (1993) 147.
[23] E.Y. Tshuva, I. Goldberg, M. Kol, J. Am. Chem. Soc. 122 (2000) 10706.
[24] (a) J.D. Scollard, D.H. McConville, J. Am. Chem. Soc. 118 (1996) 10008;
(b) R. Baumann, W.M. Davis, R.R. Schrock, J. Am. Chem. Soc. 119 (1996) 3831.
[25] C. Lorber, F. Wolff, R. Choukroun, L. Vendier, Eur. J. Inorg. Chem. (2005) 2850.
[26] U. Christmann, H. Dau, M. Haumann, E. Kiss, P. Liebisch, D. Rehder, G. Santoni, C. Schulzke, Dalton Trans. (2004) 2534.
[27] E.Y. Tshuva, I. Goldberg, M. Col, Organometallics 20 (2001) 3017.
[28] G.M. Sheldrick, Acta Cryst. A 46 (1990) 467.
[29] G.M. Sheldrick, T.R. Schneider, Methods Enzymol. 277 (1997) 319.
[30] M. Nardelli, Comp. Chem. 7 (1983) 95.
[31] M.N. Burnett, C.K. Johnson, ORTEP-III: Oak Ridge Thermal Ellipsoid Plot Program for Crystal Structure Illustrations, Report ORNL-6895, Oak Ridge National Laboratory, Oak Ridge, TN, USA, 1996.
[32] S. Groyasman, I. Goldberg, Z. Goldschmidt, M. Kohl, Inorg. Chem. 44 (2005) 5073.
[33] (a) F. Wolff, C. Lorber, R. Choukroun, B. donnadieu, Inorg. Chem. 42 (2003) 7839;
(b) D. Maity, A. Ray, W.S. Sheldrick, H. Mayer Figge, B. Bandyopadhyay, M. Ali, Inorg. Chim. Acta 359 (2006) 3197.
[34] M. Ali, A. Ray, W.S. Sheldrick, H. Mayer-Figge, S. Gao, A.I. Shames, New J. Chem. 28 (2004) 412, and the references therein.
[35] (a) T.K. Paine, T. Weyhermüller, E. Bill, E. Bothe, P. Chaudhuri, Eur. J. Inorg. Chem. (2003) 4299;
(b) G. Asgedom, A. Sreedhara, C.P. Rao, Polyhedron 14 (1995) 1873;
(c) G. Asgedom, A. Sreedhara, J. Kivikoski, J. Valkonen, E. Kolehmainen, C.P. Rao, Inorg. Chem. 35 (1996) 5674.